J. Chem. Sci. Vol. 124, No. 6, November 2012, pp. 1217–1228.

Cu(II) complexes of glyco-imino-aromatic conjugates in DNA binding, plasmid cleavage and cell cytotoxicity

AMIT KUMAR[a], ATANU MITRA[b], AMRENDRA KUMAR AJAY[c], MANOJ KUMAR BHAT[c] and CHEBROLU P RAO[a,b,*]

[a]Department of Biosciences and Bioengineering, [b]Department of Chemistry, Indian Institute of Technology Bombay, Powai, Mumbai 400 076, India

[c]National Centre for Cell Science, Ganeshkhind, Pune 411 007, India

e-mail: cprao@iitb.ac.in

Abstract. Binding of metal complexes of C2-glucosyl conjugates with DNA has been established by absorption and fluorescence studies. Conformational changes occurred in DNA upon binding have been studied by circular dichroism. All these studies are suggestive that the metal complexes bind to DNA through intercalation. Binding of di-nuclear copper complex **5** was found to be stronger when compared to the other complexes studied. Copper complexes were found to cleave the plasmid DNA in the absence of oxidizing or reducing agent, whereas, zinc complexes do not cleave. Metal complexes have shown toxicity to the HeLa and MCF–7 cell lines. Morphological studies, western blot and FACS analysis are suggestive of apoptotic cell death induced by the metal complexes. Di-nuclear copper complexes were found to be better as compared to the mononuclear ones in binding, plasmid cleavage and also in causing more cell death.

Keywords. Glyco-metal-complexes; DNA cleavage; cytotoxicity; apoptosis.

1. Introduction

Metal complexes having the ability to bind and cleave double stranded DNA under physiological conditions are of great importance because of their applicability as drugs.[1–4] Platinum-based drugs are most widely studied and these interact with DNA mainly through the formation of intra-strand GpG cross-linked adducts located in the major groove which in turn is responsible for their antitumour properties.[3] However, the platinum-based drugs suffer from their severe toxicity. So the interest has been focused to the other metal-based drugs which bind DNA.[5–18] The effect of the metal-based drug is also being internally modulated owing to the type of organic molecular frame work that wraps the metal ion centre, since such molecular skeleton would involve in a direct interaction with the DNA or cell surface. In this context, glycoconjugates would be of great relevance and importance owing to their interacting ability with the DNA, their water solubility and their biological benign nature. Therefore, the present paper deals with the DNA binding, plasmid cleavage and cytotoxicity of the Cu(II) complexes of glyco-imino-aromatic conjugates, while the precursor ligands and their Zn(II) complexes act as control systems. Toxicity of metal complexes was compared with the carbo-platin and found that these are more effective.

*For correspondence

2. Experimental

2.1 *Synthesis and characterization*

The glyco-imino-aromatic conjugates, viz., **1** and **2**, were synthesized as reported by us earlier.[19–22] The metal ion complexes of glyco-imino-aromatic conjugates were synthesized as reported in this section.

2.1a *Synthesis of mononuclear Cu(II) complex of **1** (**3**)*: A 0.28 g of **1** was suspended in 20 ml of THF and to this 0.19 g of $Cu(OAc)_2.H_2O$ in 10 ml of water was added. The solution turns dark green immediately. This was then refluxed for 6 h at 70°C and was then brought to the room temperature. At this stage the reaction mixture was kept at 4°C for 3 days and the solid product precipitated was filtered and washed several times with fractions of ice cold ethanol and finally with diethylether and then dried under vacuum. IR (KBr); 3418, 3294 (m) $\upsilon_{(O-H)}$ and $\upsilon_{(N-H)}$ 2925 and 2872 $\upsilon_{(C-H)}$, 1618 $\upsilon_{(C=N)}$ cm^{-1}; Anal Calcd for $C_{17}H_{23}CuNO_7$: C, 48.97; H, 5.56 and N, 3.36; Found C 44.89, H, 5.38 and N, 3.29; MALDI-TOF: m/z 416 $[M]^+$ (30%), 832 $[2M]^+$ (20%).

2.1b *Synthesis of di-nuclear Cu(II) complex of **1** (**4**)*: A 0.28 g of **1** was suspended in ethanol and to this

a 0.2 g of $Cu(OAc)_2.H_2O$ in 5 ml of water was added and the resulting solution was refluxed at 80°C for 12 h. Then the mixture was stirred at room temperature for 24 h followed by storing at 4°C. The solid product precipitated was filtered and washed several times with fractions of ice cold ethanol and finally with diethylether and dried under vacuum. IR (KBr); 3416, 3352 (m) $\upsilon_{(O-H)}$ and $\upsilon_{(N-H)}$ 2924 and 2851 $\upsilon_{(C-H),}$ 1617 $\upsilon_{(C=N)}$ cm^{-1}; Anal Calcd for $C_{26}H_{30}Cu_2N_2O_{12}$: C, 45.28; H, 4.38 and N, 4.06; Found C 45.18, H, 4.32 and N, 4.31; MALDI-TOF: m/z 688 $[M]^+$.

2.1c *Synthesis of dinuclear Cu(II) complex of **2** (**5**)*: The compound was synthesized following the procedure given in case of dinuclear Cu(II) complex **4**. IR (KBr); 3423 (m) $\upsilon_{(O-H)}$ and $\upsilon_{(N-H)}$ 2924 and 2853 $\upsilon_{(C-H),}$ 1619 $\upsilon_{(C=N)}$ cm^{-1}; Anal Calcd for $C_{34}H_{34}Cu_2N_2O_{12}$: C, 51.71; H, 4.34 and N, 3.55; Found C 52.01, H, 4.32 and N, 3.56; MALDI-TOF: m/z 790 $[M+H]^+$.

2.1d *Synthesis of mononuclear Zn(II) complex of **1** and **2** (**6** and **7**)*: A 0.22 g of $Zn(OAc)_2.2H_2O$) in 5 ml water was added to a suspension of the glycoconjugate (0.28 g of **1** or 0.34 g of **2**) in methanol. The mixture was refluxed at 70°C for 10 h and then stirred at room temperature for 24 h. Then the solution was stored at 4°C for 2–3 days. The solid product was separated by filtration and was washed with ice cold ethanol followed by fractions of diethylether, and dried under vacuum. The products were characterized. Data for **6**: IR (KBr); 3358 (m) $\upsilon_{(O-H)}$ and $\upsilon_{(N-H)}$ 2935 and 2770 $\upsilon_{(C-H),}$ 1637 $\upsilon_{(C=N)}$ cm^{-1}; FAB-MS: m/z 346 $[M]^+$; Anal calcd for $C_{13}H_{16}NO_6Zn$: C, 44.91; H, 4.64; N, 4.03, Found C, 44.59; H, 4.97; N, 3.92. Data for **7**: IR (KBr); 3445 (m) $\upsilon_{(O-H)}$ and $\upsilon_{(N-H)}$ 2925 and 2854 $\upsilon_{(C-H),}$ 1621 $\upsilon_{(C=N)}$ cm^{-1}; Anal. calcd. For $C_{17}H_{19}O_6N.C_4H_6O_4.Zn$: C, 48.21; H, 5.03; N, 2.14 found C, 48.26; H, 5.55; N, 2.68. FAB-MS: m/z 397 $[M]^+$.

2.2 *Absorption spectroscopy*

Absorption studies were carried out in 25 mM Tris buffer at pH = 7.4. In one experiment, the absorption peak of DNA was monitored by keeping the CT–DNA concentration constant (30 μg/ml) and varying the concentration of the metal complex (2.5 μl of 10 mM). In another experiment, the absorption bands of the complexes were monitored. The complexes were titrated with continuous addition of 2 μl of CT–DNA (200 μg/ml).

2.3 *Fluorescence spectroscopy*

In a typical fluorescence experiment, DNA (30 μl of 1 mg/ml) and ethydium bromide (EtBr, 10 μl of 1 mg/ml) were taken. Sample was excited at 497 nm for EtBr. In the titration experiment, 2.5 μl of either the glycoconjugate or its metal complex (10 mM) was added and the spectra were recorded after each addition. All the experiments were carried out in 25 mM Tris buffer at pH = 7.4. Spectrum of EtBr titrated with metal complexes have been subtracted for further analysis.

2.4 *Thermal denaturation study*

Thermal denaturation studies were carried out on a Shimadzu UV–2101PC equipped with Julabo F 25 temperature controlling unit. The absorbance at 260 nm was continuously monitored for solutions of CT–DNA (30 μg) in the absence and in the presence of the metal complex (5 μM) over a temperature range of 25 to 100°C. The experiment was carried out in 25 mM Tris buffer of pH = 7.4 without NaCl. Sample was incubated at a particular temperature for 5 min before recording the spectrum.

2.5 *Circular dichroism studies*

CD spectra were recorded at 25°C on a Jasco–J–815 spectropolarimeter at a scan speed of 40 nm/min with a response time of 4 s and a slit width of 1.5 nm. Quartz cell of 2 mm path length was used for the measurements in 190–300 nm range. All the measurements were made at a fixed CT–DNA concentration of 30 μg/ml in 5 mM Tris buffer pH = 7.4. Each spectrum reported is an average of four successive scans. Either the buffer or the metal-complex recorded under the same conditions was subtracted from the main titration spectrum before interpreting the data.

2.6 *Plasmid DNA cleavage studies*

All the DNA cleavage studies were carried out in 25 mM Tris buffer of pH = 7.4 at 37°C with constant shaking at ∼300 rpm. Since, complexes are partially soluble in the buffer system, the complex was first dissolved in DMSO and the DNA cleavage studies were carried out (in the absence of any oxidant/co-oxidant) by mixing the DNA (pBR322) and metal complexes. In a typical DNA cleavage experiment, a mixture of metal complex (∼30–50 μM) and plasmid DNA were incubated, and 10 μl of the reaction mixture was taken out at

different time intervals from 0 to 180 min. The reaction was stopped by the addition of sample loading buffer. Samples were run on 1% agarose gel.

2.7 *Cell lines*

Cervical carcinoma cells, HeLa, breast cancer cells, MCF–7 were purchased from ATCC (Manassasas, VA, USA) and were maintained in National Cell Repository at NCCS, Pune, India. Cell lines were cultured in Dulbecco's Modified Eagle Medium (DMEM) supplemented with 10% heat inactivated (56°C for 30 min) fetal bovine serum (FBS) at 37°C in humidified chamber with 5% CO_2.

2.8 *Cell proliferation assay*

The cell proliferation was determined by methylthiazole tetrazolium (MTT) assay.[23,24] In this assay, the conversion of yellow tetrazole [3-(4,5-Dimethylthiazol-2-yl)-2,5-diphenyltetrazolium bromide, MTT] into the purple formazan by the activity of mitochondrial reductase was monitored. In brief, the cells were treated with the complexes as per the experimental requirement and further incubated for 48 h. A 50 µL of MTT (1 mg/ml) was added to each well and incubated for 4 h at 37°C. All 100 µL of 2–propanol was added and the absorbance was measured at 570 nm using 630 nm as reference filter. Absorbance given by untreated cells was considered as 100% cell survival.

2.9 *Microscopy studies*

The cells plated in 35 mm dish were treated with different concentrations of the copper–complex and incubated for the indicated time. Then the cells were imaged by DP30 or DP71 camera attached to the fluorescence microscope (Olympus, Heidelberg, Germany) with 360 nm and 397 nm filters.

2.10 *Western blotting*

Cells were treated at the corresponding IC_{50} concentration. After 48 h of treatment, the cells were washed thrice with ice-cold phosphate buffered saline (PBS) and lysed in ice-cold lysis buffer {50 mM Tris-Cl, pH 7.5, with 120 mM NaCl, 10 mM NaF, 10 mM sodium pyrophosphate, 2 mM EDTA, 1 mM Na_3VO_4, 1 mM PMSF, 1% NP-40 and protease inhibitor cocktail}. For western blot analysis, the proteins were transferred onto the nitrocellulose membrane and were incubated with 1:1000 dilutions of primary antibodies overnight at 4°C in TBS. Thereafter, membranes were incubated with 1:2000 dilutions of HRP-linked secondary antibodies in TBS for 2 h at room temperature and the washing steps were repeated as earlier. The HRP activity was detected by chemiluminescence substrate. Blots were developed for poly ADP ribose polymerase (PARP), and glyceraldehyde 3-phosphate dehydrogenase (GAPDH) for the equal loading.

2.11 *FACS analysis*

The cells were plated at a density of 5×10^5 cells in 35 mm plates and allowed to adhere for 24 h. These were treated at IC_{50} and incubated for 48 h and were

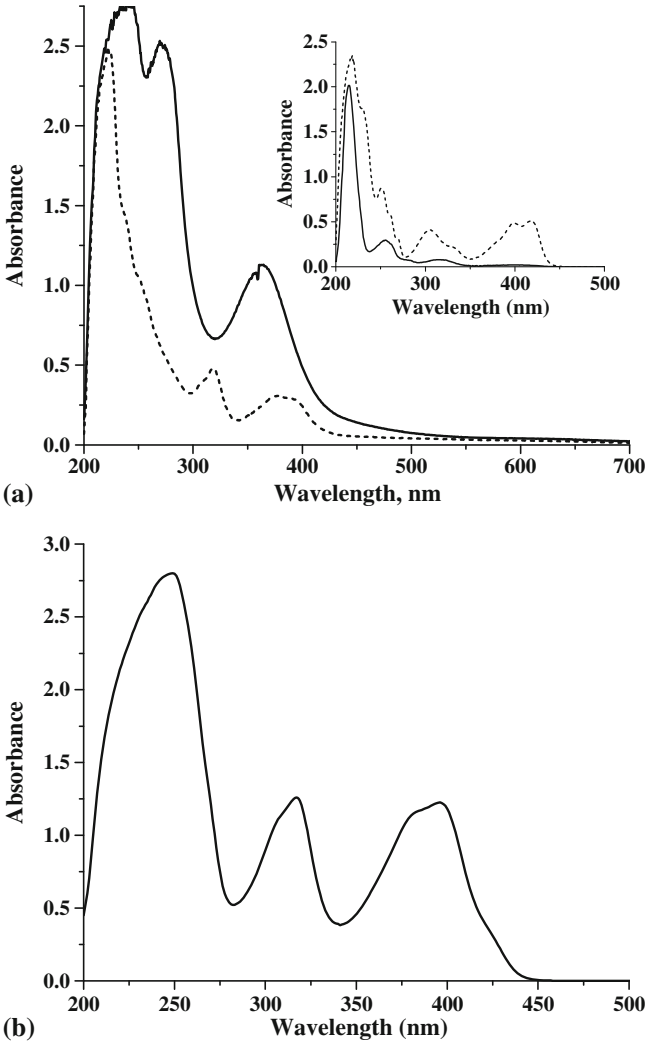

Figure 1. UV-Vis absorption spectra for: (**a**) **4** (solid line) and **5** (dotted line) and (**b**) **7**. The spectra given in the inset of (**a**) corresponds to the precursor ligands, **1** (solid line) and **2** (dotted line).

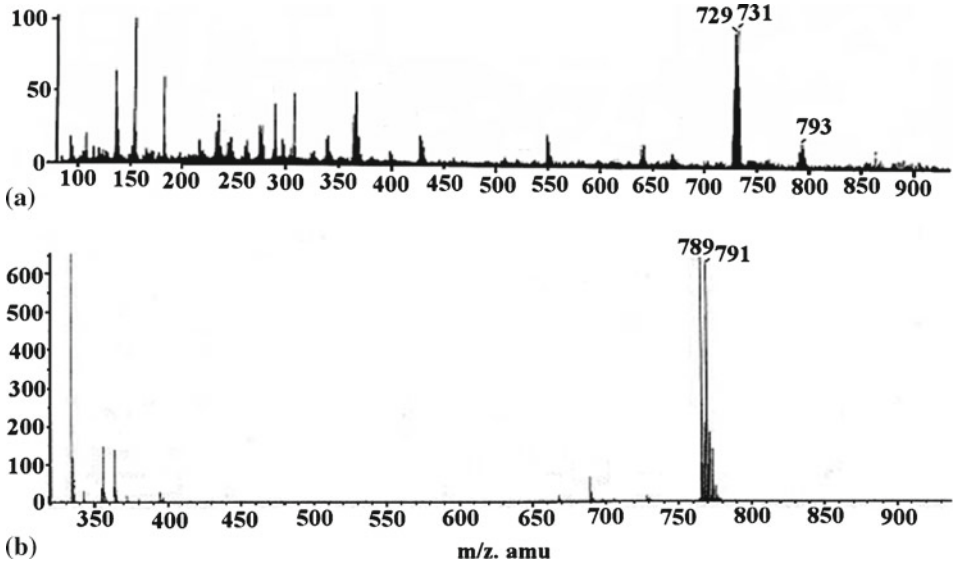

Figure 2. (**a**) FAB mass spectrum for **4**. (**b**) ESI MS spectrum for **5**.

harvested by trypsinization. The cells were fixed in ice chilled 70% ethanol and were treated with RNase (200 µg/ml) for 30 min at 37°C. Fifty µg/ml propidium iodide (PI) was added and incubated in dark for 30 min on ice. The fluorescence of PI was measured through a 585 nm filter in flow cytometer (FACS Calibur, Becton and Dickinson) for 10,000 cells. Data were analysed using cell quest software (Becton and Dickinson).

3. Results and discussion

C2-Glucosyl conjugates of salicyl- and naphthylimines (**1** and **2**) were synthesized by following the procedure reported by us earlier.[25,26] All the metal complexes (**3** to **7**) were prepared by reacting the glycoconjugates with the corresponding metal acetate and were characterized by a variety of spectral and analytical techniques as given in the experimental section. While the Cu(II) complexes, viz., **3**, **4** and **5**, are used for demonstrating their cytotoxicity aspects, the Zn(II) complexes, viz., **6** and **7**, were used as control compounds. While the elemental analysis and mass spectral data provided support for the composition of these complexes, the presence of the carbohydrate, imine and aromatic moieties could be delineated from the vibrational bands observed for O–H, N–H, C–H and C=N groups in the IR spectra. Upon coordination, the imine stretching frequency decreases indicating the involvement of this moiety in metal ion binding. Comparison of the absorption spectra of the complexes with those of the ligands clearly support the formation of the complexes. The EPR provided support for the presence of copper in its +2 oxidation state. Representative spectra of UV-Vis absorption, mass spectrometry and EPR are given in figures 1, 2 and 3, respectively. Schematic structures of all these are given in chart 1.

3.1 *UV–Visible spectroscopy*

UV–Visible spectroscopy has been performed to study the interaction of the complexes with DNA keeping the CT–DNA concentration constant (30 µg/ml) and varying the concentration of the complex (2.5 µl of 10 mM). Only marginal changes were observed in hyper chromacity of the DNA as monitored through 260 nm band in case of **4** and **5** (figure 4). The band at 260 nm resulted in K_a ($\times$ 10^3 M^{-1}) = 3.0 and 3.7 for **4** and **5**, respectively, as derived based on the Benesi–Hildebrand equation. These results suggest that the naphthyl conjugates bind better than that of their salicyl counter parts. In another experiment, the absorption

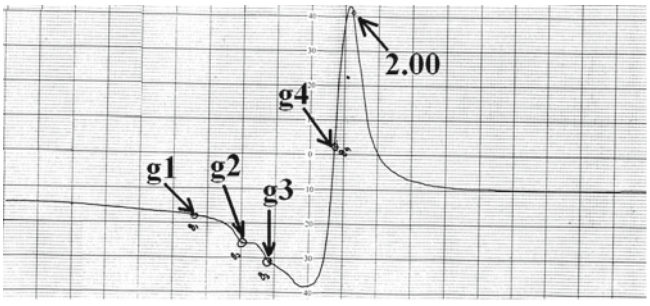

Figure 3. Powder EPR spectrum for **4**. The arrow indicates 'g' value of 2.00. The labelled 'g' values are as follows: g_1 = 2.796; g_2 = 2.476; g_3 = 2.337 and g_4 = 2.066.

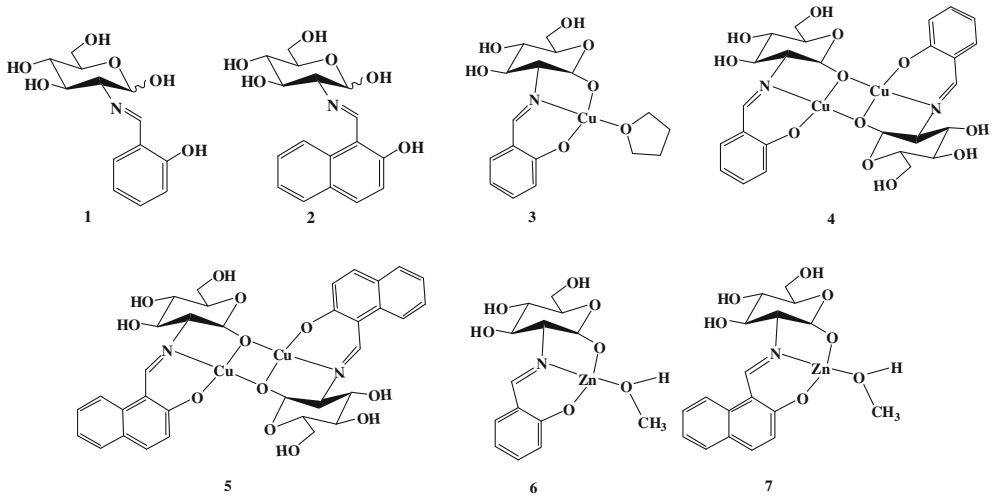

Chart 1. Schematic structures of the compounds used in the present work.

bands of the complexes were monitored by the addition of varying concentrations of DNA and found that there are significant changes in the absorbance of the 260 nm band of the complexes in the presence of DNA supporting their interaction.

The difference observed in the absorbance of the 260 nm band is much higher in case of the copper complexes (**3** and **4**) as compared to the zinc complex (**6**) as can be seen from figure 5a. The binding constants of these with the DNA were established based on this band using Benesi–Hildebrand equation and are being shown as histogram in figure 5b. The data clearly reveal that the copper complexes bind better than that of the zinc complex with CT–DNA.

The difference in the aromatic moiety, viz., from the salicilyl to naphthyl, showed no significant change in the binding strength. A 2 nm bathochromic shift was observed only in case of 260 nm band and a 50–70% hypochromism was also observed. These changes observed in the spectra were typical of a complex bound to DNA through intercalation.[27–29] Similar studies could not be carried out with **7** owing to the precipitation problems encountered at higher concentrations. On the other hand, $Cu(ClO_4)_2$ and $Zn(ClO_4)_2$, do not cause any bathochromic shift or hypochromacity when titrated with the DNA at the same concentration as control, suggesting the role of the glycoconjugate in the binding.

3.2 *Fluorescence spectral titrations*

Ethidium bromide (EtBr) – DNA mixture was used for the binding studies. During the course of the titration, it was observed that **3**, **4** and **5** quenches the fluorescence intensity of EtBr, while the precursor organic molecules, viz., **1** and **2** do not (figure 6). This is possible when a complex replaces the EtBr from its intercalation into the medium. Therefore, the present data suggest that the complexes interact with DNA through intercalating mode to different extents by using their naphthyl or salicyl aromatic moieties. However, either

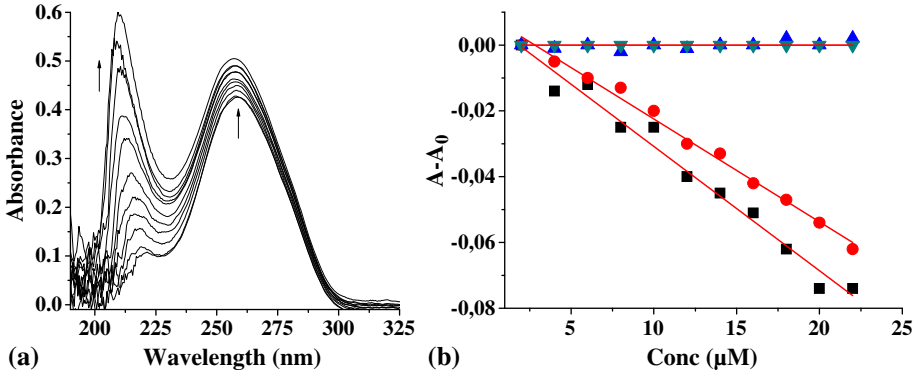

Figure 4. DNA binding studies by UV-visible spectroscopy: (**a**) Spectral traces obtained in case of **5**, (**b**) plots of absorption *vs*. conc. ▲ – 3, ● – 4, ■ – 5, and ▼ – 6.

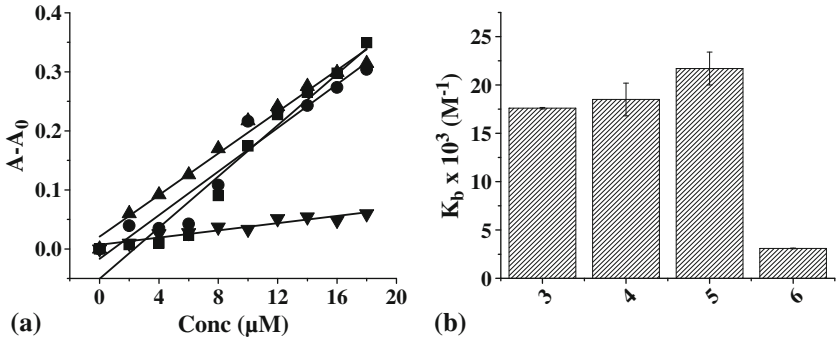

Figure 5. Binding by absorption studies (**a**) Benesi–Hildebrand plots of the binding of metal ion complexes with DNA. (**b**) Bar diagram of association constant obtained by the Benesi–Hildebrand analysis. ▲ – 3, ● – 4, ■ – 5, ▼ – 6.

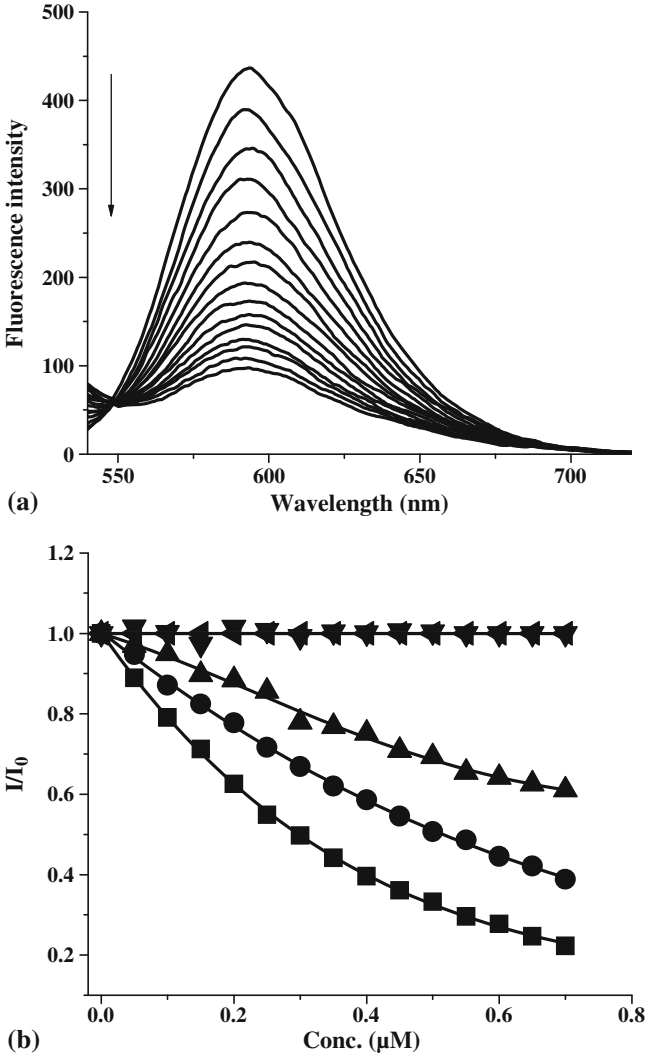

Figure 6. Fluorescence spectral traces obtained during the titration of CT–DNA and complexes: (**a**) **5** (**b**) Relative intensity plot of the titration derived from the spectral traces. ■ – 5, ● – 4, ▲ – 3, ▼ – 1, ◄ – 2.

the $Cu(ClO_4)_2$ or the simple glycoconjugate is unable to quench the fluorescence intensity of EtBr. This indicates that the metal ions as well as the organic moiety together (i.e., the complex) are required to intercalate and replace the EtBr.

The extent of fluorescence quenching has been further gauzed by comparing the concentrations at which 50% of the fluorescence is quenched (IF_{50}). The IF_{50} were found to be in the range of 0.2 to 0.9 μM for different complexes. The fluorescence quenching efficiency follows a trend, viz., **5** (0.3 μM) > **4** (0.5 μM) > **3** (0.9 μM) >>> **2** ~ **1** indicating a several fold higher quenching in case of the Cu(II) complexes as compared to the precursor organic molecular systems (**1** and **2**). The higher quenching efficiency observed with the

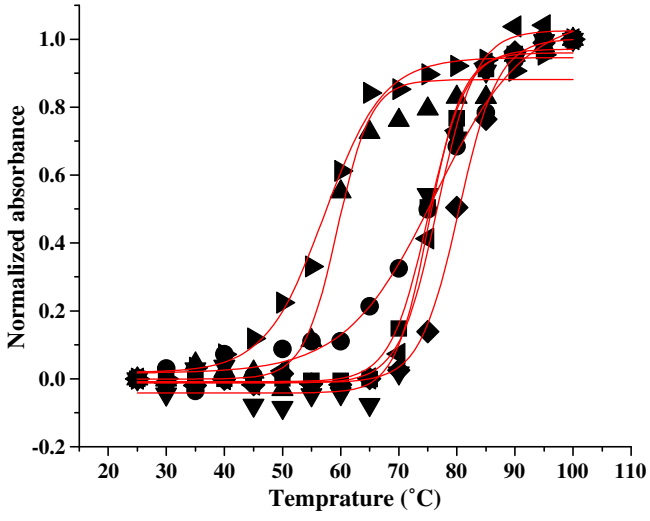

Figure 7. DNA melting curve of the CT-DNA in the presence and absence of metal complexes. Melting were recorded in the 25 mM Tris buffer pH = 7.4 with a 5°C /min^{-1}. Symbols are ■ – DNA^-, ◄ – 3, ▼ – 4, ● – 5, ► – 6, and ▲ – 7, ♦ – EtBr.

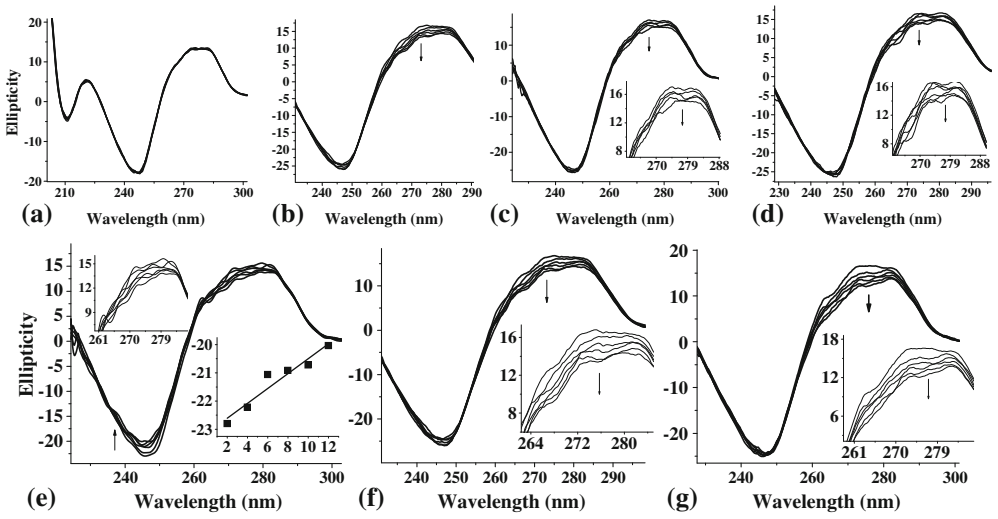

Figure 8. CD spectral traces obtained during the titration of CT–DNA with glycoconjugates and their complexes. All the CD experiments were performed in the 5 mM Tris buffer pH = 7.4: (**a**) **1**, (**b**) **2**, (**c**) **3**, (**d**) **4**, (**e**) **5**, (**f**) **6** and (**g**) **7**. Inset: showing the expanded region at base stack region. In (**e**) showing the ellipticity changes at 245 nm as a function of concentration.

naphthyl derivatives may be attributed to the larger surface area of the naphthyl moiety as compared to the salicyl one. Similarly, the dinuclear copper complex indeed exhibited a higher quenching than the mononuclear one. All these results are in conformity with that observed in the absorption spectroscopy. Fluorescence studies with Zn(II) complexes, viz., **6** and **7** could not be performed. Because, a higher amount of DNA is required to obtain considerable fluorescence intensity and also precipitation occurs in the medium upon the addition of the metal ion complex (**6** and **7**).

3.3 *Thermal denaturation studies*

The melting temperature (T_m) of DNA was determined in the presence and in the absence of the complexes by monitoring the absorbance at 260 nm as a function of the temperature (figure 7). The T_m of the CT–DNA was increased by 1–3°C when bound to the copper–complexes (**3** to **5**), suggesting a possible intercalation of the complex and thus in support of the results obtained from the absorption and fluorescence studies. However, the T_m of the DNA was found to be decreased by 10–15°C in the presence of Zn(II) complexes, suggesting the destabilization of the DNA duplex.

3.4 *Circular dichroism studies*

Circular dichroism (CD) spectra of CT–DNA gave a positive band at 275 nm due to the base stacking and a negative band at 245 nm due to helicity, which are characteristic of the right handed B form of DNA.[28] Titration of DNA with the metal complex led to a change in the helical as well as base stack region in case of **5**. Considerable changes observed in the ellipticity are indicative of the intercalative nature of the

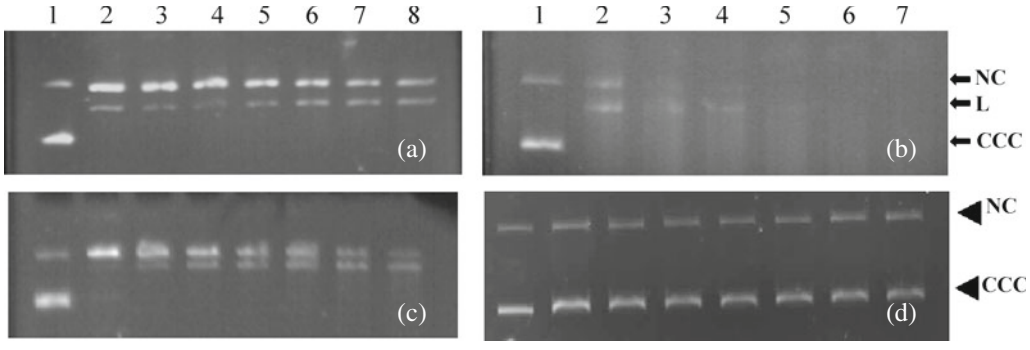

Figure 9. Cleavage studies of pBR322 in the presence of metal complex without addition of the oxidizing or reducing agents: (**a**) **3**, (**b**) **4**. (**c**) **5** and (**d**) **7.** Lane1–control, Lane 2–8 are for 5, 15, 30, 45, 60, 120, 180 min incubation.

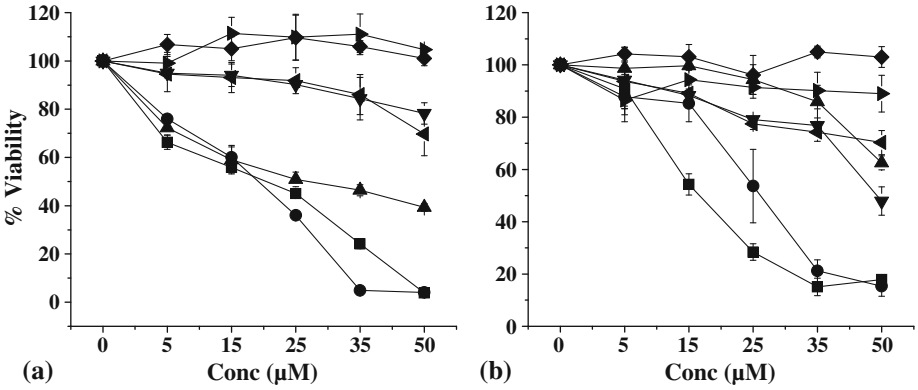

Figure 10. Dose dependent curves (percentage viability curves) of the HeLa (**a**) and MCF – 7 (**b**) cells after treatment with the metal complexes. Viability was checked by MTT assay after 48 h. ♦ – 1, ► – 2, ▲ – 3, ● – **4**, ■ – **5**, ◄ – **6**, ▼ – **7**.

complexes (figure 8). All these results are in accordance with the observed bathochromacity, displacement of EtBr and increase in the T_m, to support the intercalative binding mode of the copper complexes, particularly in case of the naphthyl conjugate, **5**. Similar results have been reported in the literature, where the changes observed in the ellipticity have been correlated with the intercalative nature of the complexes.[29]

The Zn(II) complexes, viz., **6** and **7**, also affect the base stack region (figure 8). This indicated that the metal ion complexes may bind with DNA at the base stack region. Simple glycoconjugate or $Cu(ClO_4)_2$ or $Zn(ClO_4)_2$ does not show any change either in the helical region or in the base stack region. These results are suggestive of the importance of the metal complex of the glyoconjugate in DNA binding and cleavage.

3.5 *Plasmid DNA cleavage studies*

The plasmid DNA cleavage ability of the compounds was studied by using pBR322 in the absence of any oxidant/reductant in the incubation mixture. An aliquot of 10 μl was taken out at different time points in first three hours. The samples were run on 1% agarose gel.

All the three Cu(II) complexes, viz., **3**, **4** and **5** show chemical nuclease activity. While **3** shows only the nicked circular (NC) form, complete disappearance of the covalently closed circular (CCC) form was noticed in case of **4** and **5** (figure 9). The studies revealed that the dinuclear Cu(II) complex is more active as chemical nuclease as compared to the mononuclear one. The studies performed with the organic precursor, viz., **1**, **2**, and the Zn^{2+} complexes, viz., **6** and **7**, did not show any cleavage activity of the plasmid DNA. Plasmid was found to be intact even in the presence of simple $Cu(ClO_4)_2$ and $Zn(ClO_4)_2$ salts. All these suggest that only the Cu(II) complexes are effective in cleavage, neither the ligand nor the metal ion alone.

3.6 *Cell cytotoxicity studies*

Inhibition of cell proliferation was examined by incubating cells with different concentrations of glycoconjugates, their Cu^{2+}/Zn^{2+} complexes or carboplatin for two cell cycles (48 h). Cervical cancer (HeLa) and breast cancer (MCF–7) cell lines were treated with the complexes and carboplatin in a dose dependent manner (figure 10). These complexes have a significant inhibitory effect on the proliferation of HeLa and MCF–7 cells.

Half maximal inhibitory concentration (IC_{50}) of the compounds for HeLa, and MCF–7 have been listed in table 1. The IC_{50} values are certainly lower in the present case than that exhibited by carboplatin as tested by us under similar conditions. The complex **5** showed better activity among all the complexes studied. However, **4** showed better anti–proliferative activity than

Table 1. IC_{50} values obtained after the treatment with the metal complexes.

Metal-complex	$IC_{50}(\mu M)$ HeLa	MCF–7
1	NI	NI
2	NI	NI
3	55 ± 3	50 ± 3
4	38 ± 3	24 ± 4
5	28 ± 2	14 ± 3
6	105 ± 2	81 ± 4
7	78 ± 4	64 ± 5
Carbo–Platin	243 ± 40	434 ± 67

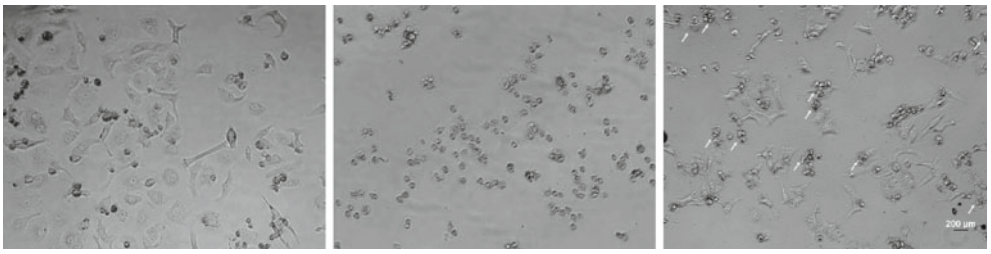

Figure 11. HeLa cells treated with **5**. (**a**) Live cell after 24 h, (**b**) dead cell after 24 h treatment, (**c**) showing the blebbing morphology of apoptotic cells.

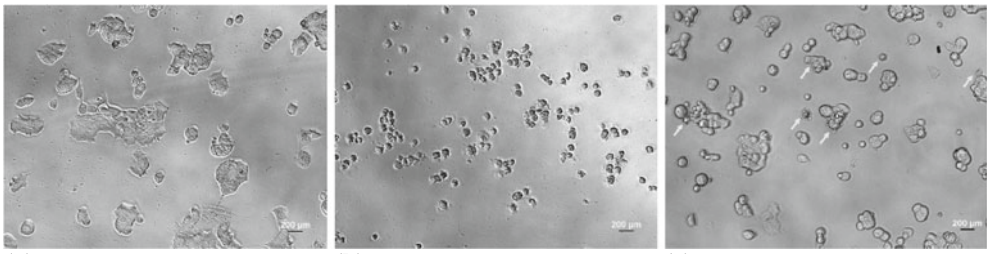

Figure 12. MCF–7 cells treated with **5**: (**a**) Live cell after 24 h, (**b**) dead cell after 24 h treatment and (**c**) showing the blebbing morphology of apoptotic cells.

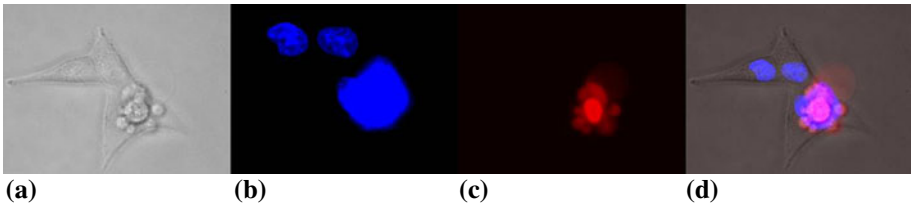

Figure 13. HeLa cells treated with **5**. Differentiation of live and dead cell based on the DAPI and PI staining: (**a**) Live cells after 24 h, (**b**) DAPI staining of live and dead cells (showing the cell blebbing of apoptotic cell death), (**c**) dead cell staining by PI of same area and (**d**) overlay of the three images.

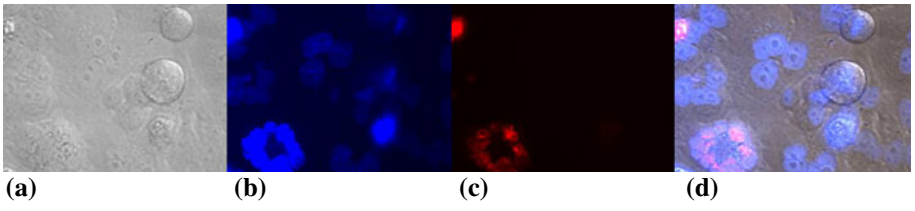

Figure 14. MCF–7 cells treated with **5**. Differentiation of live and dead cell based upon the DAPI and PI staining: (**a**) Live cells after 24 h, (**b**) DAPI staining of live and dead cells (showing the cell blebbing of apoptotic cell death), (**c**) dead cell staining by PI of same area and (**d**) overlay of the three images.

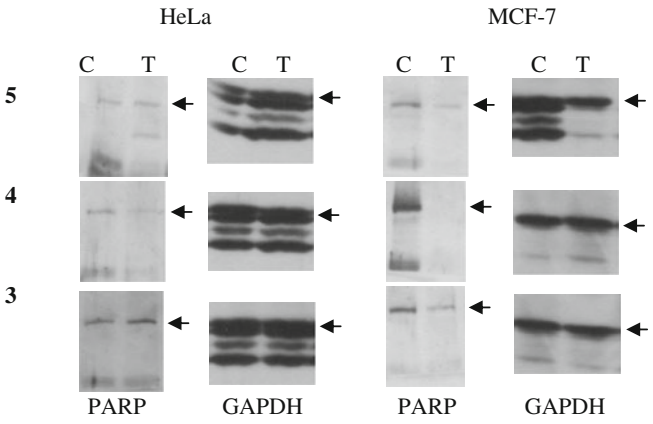

Figure 15. Western blot analysis for PARP for glycoconjugate metal complexes treated cells. C and T stand for control and treated respectively. Blots were prepared after 48 h. C – control, T – treated.

3 suggesting that a dinuclear complex is more potent than the mononuclear one. Additionally, cytotoxicity of Cu(II) complex was found to be better than the corresponding Zn(II) complex. On the other hand, sample **1** or **2** or $Cu(ClO_4)_2$ or $Zn(ClO_4)_2$, do not exhibit any appreciable cytotoxicity. All these clearly suggest that the presence of a metal ion complex is required for the cell toxicity, that too a copper complex. Copper complexes are not uncommon in the literature for their cytotoxicity effect.[30–34]

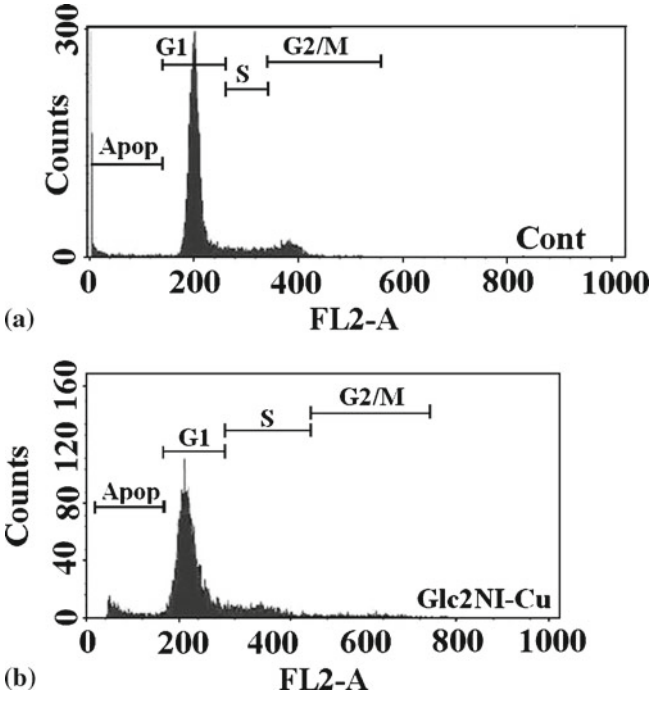

Figure 16. FACS analysis of the MCF–7 cell. (**a**) Control untreated cells, (**b**) treated with the **5**. FACS was carried out after the 48 h treatment at indicated IC_{50} concentration. Cells were stained with the PI.

3.7 *Morphological studies of the treated cells*

The cells treated with the complexes were studied using phase contrast and fluorescence microscopy for their morphological changes. Toxicity of cells was observed after 24 h (figures 11 and 12). Many of the cells show the characteristics of the cells undergoing apoptosis. A series of biochemical events are known in the literature to lead to morphological changes, viz., blebbing, loss of membrane asymmetry and attachment, cell shrinkage, nuclear fragmentation, chromatin condensation, and chromosomal DNA fragmentation. Features such as blebbing, cell shrinkage were also observed in case of HeLa and MCF–7 cells when treated with **5** (figures 11 and 12).

The live and dead cells can be further differentiated by staining techniques. DAPI is a fluorescent dye which stains the live nucleus, whereas PI stains the dead cells but not the live cells. It can be seen from figures 13 and 14, that the DAPI and PI clearly differentiate the live cells from the dead ones. These results are further supportive of the cell toxicity induced by the metal–ion complexes and apoptotic cell death.

3.8 *Western blot analysis*

To understand the molecular mechanism underlying the cytotoxicity of different cell lines, the levels of different proteins involved in the apoptosis have been investigated. In particular, Poly (ADP–ribosyl) polymerase (PARP) molecules were analysed by western blot analysis by comparing with the glyceraldehyde 3–phosphate

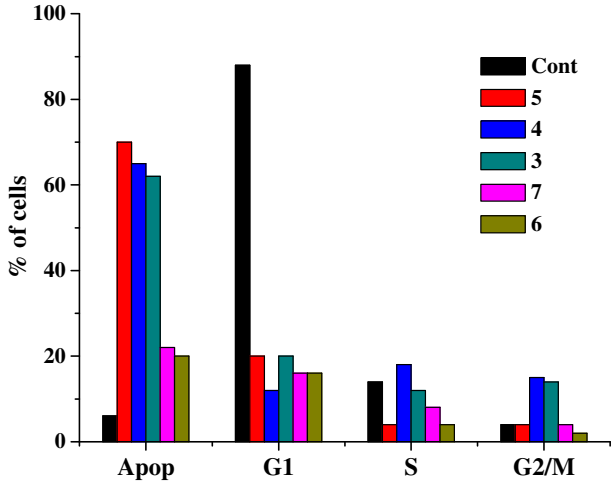

Figure 17. FACS analysis of the MCF–7 cell treated with the metal complexes. FACS was carried out after 48 h of treatment at the corresponding IC_{50} concentration.

dehydrogenase (GAPDH) as a loading control. Both the cell lines (HeLa and MCF–7) were treated at the indicated IC_{50} concentration of the complexes and blotted after 48 h. It is known that upon activation of apoptotic pathway, caspases cleave PARP into 85 and 27 kDa polypeptides. Therefore, studies were carried out to check the PARP cleavage upon complex treatment. Western blot showed the degradation of PARP protein as compared to the controlled untreated cells (figure 15). HeLa cells treated with **3** do not show any significant change in the PARP level. However, we could find 85 kDa PARP cleaved fragment only in case of HeLa cells treated with **5**. It appears that the Cu^{2+} complexes induce apoptosis by caspases activation. Caspase activation followed by PARP cleavage is intracellular sign of activation of the apoptotic machinery.

3.9 *Flow cytometric analysis*

Changes in the cell cycle distribution were monitored by flow cytometry. Cell lines (HeLa and MCF–7) were treated at the indicated IC_{50} concentration of the metal ion complexes. Cells were fixed and stained with PI, and the DNA contents were analysed by flow cytometry after 48 h. The Cu^{2+} treatment resulted in an increase in the distribution of cells at sub–G1 peak or the apoptosis peak (figures 16 and 17). These results are in agreement with the western blot analysis where the cleavage in the PARP was observed as a consequence of the activation of apoptotic cell death.

4. Conclusions

The absorption studies suggest the binding of the complexes to DNA with considerable association constants. Hyperchromacity in the DNA band and hypochromacity in the band of the complexes are indicative of the intercalative interaction of the Cu(II) complexes with DNA. These results were further supported by the competitive/displacement experiment carried out in the presence of EtBr using fluorescence emission. Marginal increase observed in the melting temperature (T_m) in the presence of metal complexes is suggestive of the DNA intercalation by stabilizing the base stack. Changes observed in the CD signature at the helical and base stack region of CT–DNA are further supportive of the winding of DNA by the complex through intercalation. The higher association constant of the complex suggests the replacement of the EtBr, causing conformational changes leading to winding the DNA and increase in the thermal denaturation temperature. All these results are in agreement with each other and support the binding of the complex through intercalation. Copper complexes cleave the plasmid DNA at as low as ~30 to 50 μM in the absence of oxidizing/reducing agent or laser/UV–visible light. The complexes were found to be significantly toxic for HeLa and MCF–7 cancerous cell lines. Cytotoxicity observed in the present case is at much lower (IC_{50}) when compared to the carboplatin, and this may qualify these complexes to be better ones as compared to those reported in the literature. The induced apoptosis by these complexes in HeLa and MCF–7 cells is PARP dependent. These results are further supported by the flow cytometric analysis. To our knowledge, these are the first Cu-based metal complexes bearing the glyco-skeletal system, showing the DNA cleavage without any external additives and exhibit considerable antiproliferative activity in the cancer cells. Although the cytotoxicity is relatively low, it is interesting to note that the Cu–glyco complexes are able to exhibit anticancer activity. Also, high toxicity might not be expected as the glyco-skeletal system is biologically benign and compatible.

References

1. Liu H-K and Sadler P J 2011 *Acc. Chem. Res.* **44** 349
2. Erkkila K E, Odom D T and Barton J K 1999 *Chem. Rev.* **99** 2777
3. Jamieson E R and Lippard S J 1999 *Chem. Rev.* **99** 2467
4. Chifotides H T and Dunbar K R 2005 *Acc. Chem. Res.* **38** 146
5. Farrer N J, Salassa L and Sadler P J 2009 *Dalton Trans.* 10690
6. Henderson W, Nicholson B K and Tiekink E R T 2006 *Inorg. Chim. Acta* **359** 204
7. Quiroga A G and Ranninger C N 2004 *Coord. Chem. Rev.* **248** 119
8. Aguirre J D, Angeles-Boza A M, Chouai A, Turro C, Pellois J-P and Dunbar K R 2009 *Dalton Trans.* 10806
9. Liu Y-C, Chen Z-F, Liu L-M, Peng Y, Hong X, Yang B, Liu H-G, Liang H and Orvig C 2009 *Dalton Trans.* 10813
10. Liu Z, Habtemariam A, Pizarro A M, Fletcher S A, Kisova A, Vrana O, Salassa L, Bruijnincx P C A, Clarkson G J, Brabec V and Sadler P J 2011 *J. Med. Chem.* **54** 3011
11. Liu Z, Salassa L, Habtemariam A, Pizarro A M, Clarkson G J and Sadler P J 2011 *Inorg. Chem.* **50** 5777
12. Ruiz J, Rodriguez V, Cutillas N, Espinosa A and Hannon M J 2011 *Inorg. Chem.* **50** 9164
13. van Rijt S H, Mukherjee A, Pizarro A M and Sadler P J 2010 *J. Med. Chem.* **53** 840
14. Gottschaldt M, Pfeifer A, Koth D, Görls H, Dahse H-M, Möllmann U, Obatad M and Yano S 2006 *Tetrahedron* **62** 11073

15. Noguchi R, Hara A, Sugie A and Nomiya K 2006 *Inorg. Chem. Commun.* **9** 355
16. Coyle B, McCann M, Kavanagh K, Devereux M, McKee V, Kayal N, Egan D, Deegan C and Finn G J 2004 *J. Inorg. Biochem.* **98** 1361
17. Abuskhuna S, Briody J, McCann M, Devereux M, Kavanagh K, Fontecha J B and McKee V 2004 *Polyhedron* **23** 1249
18. Tsyba I, Mui B B, Bau R, Noguchi R and Nomiya K 2003 *Inorg. Chem.* **42** 8028
19. Kumar A, Singhal N K, Ramanujam B, Mitra A, Rameshwaram N R, Nadimpalli S K, Rao C P 2009 *Glycoconjugate J.* **26** 495
20. Kumar A, Ramanujam B, Singhal N K, Mitra A, Rao C P 2010 *Carbohydrate Res.* **345** 2491
21. Singhal N K, Ramanujam B, Mariappandar V, Rao C P 2006 *Org. Lett.* **8** 3525
22. Ahuja R, Singhal N K, Ramanujam B, Ravikumar M, Rao C P 2007 *J. Org. Chem.* **72** 3430
23. Singh S, Upadhyay A K, Ajay A K, Bhat M K 2007 *FEBS Lett.* **581** 289
24. Kumar A, Chinta J P, Ajay A K, Bhat M K and Rao C P 2011 *Dalton Trans.* 2011 **40** 10865
25. Mitra A, Chinta J P and Rao C P 2010 *Tetrahedron Lett.* **51** 139
26. Mitra A, Hinge V K, Mittal A, Bhakta S, Guionneau P and Rao C P 2011 *Chem. Eur. J.* **17** 8044
27. Chan H L, Liu H Q, Tzeng B C, You Y S, Peng S M, Yang M and Che C M 2002 *Inorg. Chem.* **41** 316
28. Selvakumar B, Rajendiran V, Maheswari P U, Stoeckli-Evans H and Palaniandavar M 2006 *J. Inorg. Biochem.* **100** 316
29. Kelly J, Tossi A, McConnell D and Uigin O 1985 *Nucleic Acid Res.* **13** 6017
30. Loganathan R, Ramakrishnan S, Suresh E, Riyasdeen A, Akbarsha M A and Palaniandavar M 2012 *Inorg. Chem.* **51** 5512
31. Ramakrishnan S, Rajendiran V, Palaniandavar M, Periasamy V S, Srinag B S, Krishnamurthy H and Akbarsha M A 2009 *Inorg. Chem.* **48** 1309
32. Maheswari P U, van der Ster M, Smulders S, Barends S, van Wezel G P, Massera C, Roy S, Dulk H D, Gamez P and Reedijk J 2008 *Inorg. Chem.* **47** 3719
33. Aliaga-Alcalde N, Marqués-Gallego P, Kraaijkamp M, Herranz-Lancho C, Dulk H D, Gorner H, Roubeau O, Teat S J, Weyhermuller T and Reedijk J 2010 *Inorg. Chem.* **49** 9655
34. Maheswari P U, Roy S, Dulk H D, Barends S, Wezel G V, Kozlevcar B, Gamez P and Reedijk J 2006 *J. Am. Chem. Soc.* **128** 710